A Magnetic Gram Stain for Bacterial Detection**

*Ghyslain Budin, Hyun Jung Chung, Hakho Lee, and Ralph Weissleder**

Bacterial cell walls are made up of peptidoglycans (polysaccharides crosslinked by unusual peptides) in addition to other components.[1] Bacteria are often classified into Gram-positive and Gram-negative strains by their visual staining properties using crystal violet (CV), a triarylmethane dye.[2] Herein we show that bioorthogonal modification of crystal violet with *trans*-cyclooctene can be used to render Gram-positive bacteria magnetic. This modification allows for class-specific automated magnetic detection, magnetic separation, or other magnetic manipulations.

The Gram stain is one of the most commonly used tools for detecting and differentiating bacteria. The method is routinely used for clinical diagnostic purposes, as well as detecting bacteria in environmental samples. The procedure involves staining bacterial samples with crystal violet, which binds to the peptidoglycan layer of Gram-positive and Gram-negative bacteria (Figure 1). Subsequent treatment with iodine solution results in crystal violet to form an insoluble complex. Gram-positive bacteria have a thick peptidoglycan layer, whereas Gram-negative bacteria only have a thin peptidoglycan layer covered by lipopolysaccharides and lipoproteins. Upon decolorization with alcohol or acetone, only Gram-positive bacteria remain purple, while Gram-negative bacteria loose the purple color.[3–5] Despite the simplicity and robustness of the staining procedure, the final detection still relies on optical microscopy, which is often susceptible to user-dependent sampling error. Strategies for quantitative and automated detection are highly desirable, especially for the diagnosis of infectious pathogens.

Magnetic, rather than optical, labeling and detection are advantageous because of their high sensitivity and ability to diagnose crude specimens without major purification.[6] For example, one could envision rapid and sensitive detection of bacterial samples in point-of-care settings by using a miniaturized micro nuclear magnetic resonance (µNMR) device.[7,8] Direct bacterial detection by µNMR is a sensitive diagnostic method[9] and potentially allows the exclusion of culturing steps and thus minimizes the time required for
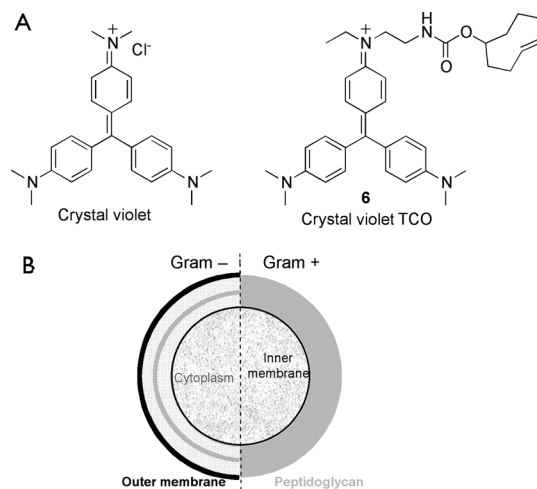

Figure 1. A) Chemical structure of crystal violet (left) and the new bioorthogonal crystal violet TCO (right). B) General composition of Gram-positive and Gram-negative cell walls.

diagnosis. Alternative magnetic detection devices include giant magnetoresistance,[10] or Hall sensors.[11] Furthermore, rendering bacteria magnetic also has implications for magnetic separation,[11,12] cell sorting,[13] magnetic force microscopy[14] or micromanipulation and force measurements using magnetic tweezers.[15]

We hypothesized that orthogonal triarylmethane-dye derivatives could be used as affinity ligands to bioorthogonally couple magnetic nanomaterials onto Gram-positive bacteria. We thus developed a crystal violet modified with *trans*-cyclooctene (CV-TCO). We show that this reagent can be used for staining Gram-positive bacteria similar to the native crystal violet. Importantly, the CV-TCO can also serve as an anchor to attach tetrazine (Tz)-modified magnetic nanoparticles (or other Tz-derivatized reporters). The developed magnetic Gram stain method was then used to enable highly sensitive detection of Gram-positive pathogens by µNMR.

Crystal violet (CV; 4,4′,4″-dimethylaminotriphenylmethane) is a deep purple dye. We sought to develop a chromophore derivative where one of the anilino moieties is modified with a *trans*-cyclooctene (TCO) orthogonal group. We started the synthesis by the condensation of two equivalents of dimethylaniline with *para*-nitrobenzaldehyde under microwave (MW) irradiation at 90 °C for four minutes in the presence of a catalytic amount of aniline (Scheme 1).[16] The aromatic nitro group was then reduced quantitatively by hydrogenolysis in presence of activated palladium affording the free amine **2** (Scheme 1). However, the formed adduct instantaneously oxidizes in presence of air, thus rendering purification and further conjugation difficult. The oxidation
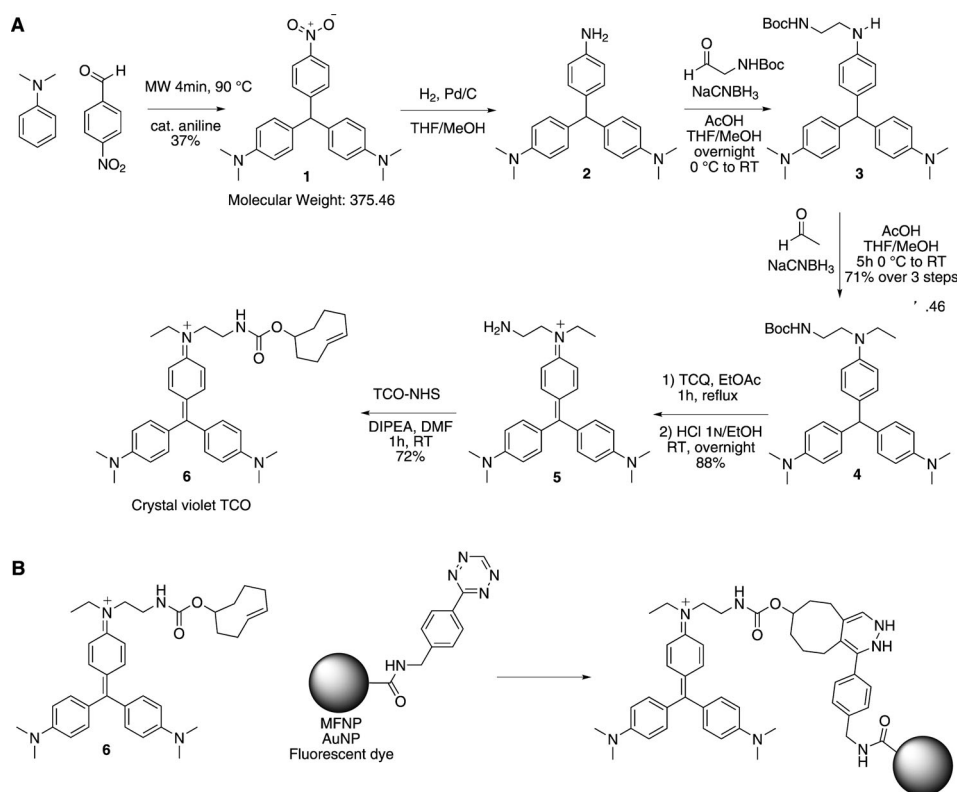
[*] Dr. G. Budin,[+] Dr. H. J. Chung,[+] Prof. H. Lee, Prof. R. Weissleder
Center for Systems Biology, Massachusetts General Hospital
185 Cambridge Street, Boston, MA 02114 (USA)
E-mail: rweissleder@mgh.harvard.edu

Prof. R. Weissleder
Department of Systems Biology, Harvard Medical School
200 Longwood Avenue, Boston, MA 02115 (USA)

[+] These authors contributed equally to this work.

Scheme 1. A) Synthesis of the bioorthogonal CV-TCO (**6**). B) Bioorthogonal reaction between CV-TCO (**6**) and tetrazine-conjugated probes (not all isomers shown). NHS = *N*-hydroxysuccinimide, DIPEA = diisopropylethylamine, Boc = *tert*-butyloxycarbonyl, TCQ = tetrachloroquinone, MFNP = magnetofluorescent nanoparticle.

process is readily apparent since the oxidized compound has an intense purple color. To avoid oxidation to the cationic dye, the aniline was therefore derivatized twice to be stable under oxygen. We thus explored the synthesis of the disubstituted aniline **4** by using a multi-step one-pot synthetic sequence. The nitro compound **1** was reduced by hydrogenation and reaction progress was followed by LC–MS (Figure S1 in the Supporting Information). After completion of the reaction, the flask was purged with argon and the free aniline was engaged in a reductive amination with Boc-2-aminoacetaldehyde, sodium cyanoborohydride, and acetic acid and stirred until completion. The secondary amine **3** underwent a classic reductive amination with acetaldehyde, sodium cyanoborohydride, and acetic acid for 5 h yielding compound **4** in 71% yield over three steps. Structure and purity of **4** were confirmed by ^{1}H NMR spectroscopy showing the characteristic chemical shift of the methylene proton at $\delta = 5.30$ ppm (see the Supporting Information). Compound **4** was then oxidized with tetrachloroquinone (TCQ) in ethyl acetate that was heated to reflux, and the formation of an intense blue indicated the formation of the cationic dye. After removal of the Boc group under acidic conditions, compound **5** was isolated and purified on neutral alumina. Finally, the free amine **5** was treated with TCO-NHS, thereby furnishing **6** (CV-TCO) with an overall yield of 17% over seven steps (Scheme 1A).

The molar extinction coefficient of CV-TCO (**6**) was $\varepsilon_{592} = 133\,013$ L mol^{-1} cm^{-1} as compared to unmodified CV, which

had $\varepsilon_{592} = 89\,146$ L mol^{-1} cm^{-1}. These results suggest that the TCO linker modification only minimally affects the molar absorptivity of the triarylmethane dye and that the bioorthogonal compound can likewise be used for Gram staining (Figure S2 in the Supporting Information). We then investigated the cycloaddition of **6** with a fluorescently labeled tetrazine, fluorescein–tetrazine (Fluo-Tz). After mixing the two compounds (0.25 mm), stirring for two minutes, the sample was analyzed by high-performance liquid chromatography–mass spectrometry (HPLC–MS). HPLC–MS spectra confirmed rapid and quantitative conversion of Fluo-Tz to the cycloaddition product without any side products (Scheme 1B and Figure S3 in the Supporting Information).

We next evaluated the efficacy of CV-TCO as a staining agent for Gram-positive bacteria. Three representative samples were prepared: *Staphylococcus aureus* (*S. aureus*; Gram-positive), *Escherichia coli* (*E. coli*; Gram-negative), and the mixture of both bacterial species. Bacterial smears on glass slides were stained with a solution of CV-TCO (1 mm) or CV for three minutes, followed by treatment with Gram's iodine solution for one minute, decolorization with 95% ethanol, and counterstaining with red safranin solution. Microscopy revealed that only Gram-positive *S. aureus* remained purple, while Gram-negative *E. coli* was decolorized owing to dissolution of the outer membrane (Figure 2A). The specificity of CV-TCO was further confirmed by UV/visible spectrometry; only Gram-positive bacteria showed an intense absorption at 595 nm (Figure S4 in the Supporting Information). Importantly, there was excellent correlation between CV and CV-TCO staining ($r^2 > 0.99$; Figure 2B).

We further investigated if the bacteria stained with CV-TCO could be magnetically labeled by using the TCO group. Bacteria stained with CV-TCO were incubated with magnetofluorescent nanoparticles modified with tetrazine (MFNP-Tz). Control samples were prepared by incubating unstained bacteria with MFNP-Tz. The T_2 relaxation values of samples were measured using a miniaturized μNMR system. For comparative analyses, the absorption (at 595 nm) of the same samples was also measured. Cellular relaxivity (r_2) was obtained by normalizing the measured $1/T_2$ values with bacterial concentration, and the r_2 differences (Δr_2) between targeted and control samples were calculated. We observed an excellent correlation ($r^2 > 0.9$) between the extent of Gram
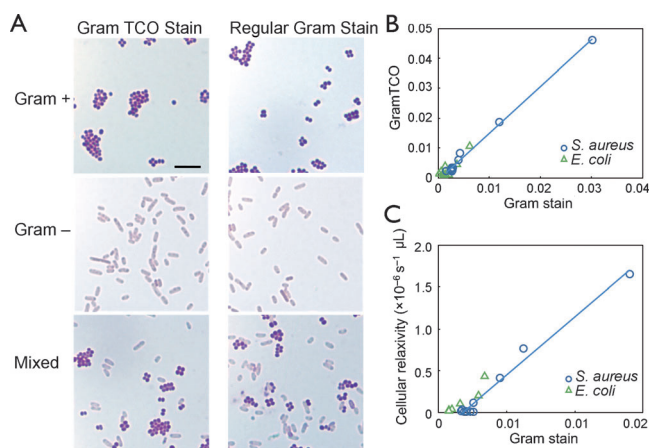
Figure 2. A) Gram staining of *S. aureus* (Gram-positive cocci), *E. coli* (Gram-negative bacilli), and mixture of *S. aureus* and *E. coli* stained with CV-TCO (left panels) or with CV (right panels; scale bar = 10 μm). B) Correlation of absorbance at 595 nm between bacteria stained with CV and CV-TCO. C) Correlation between absorbance (595 nm) and magnetic relaxivity values of bacterial cells stained with CV-TCO and labeled with magnetic MFNP-Tz.

staining and the cellular relaxivity in Gram-positive species, thereby confirming that CV-TCO on the bacterial surface was accessible for reaction with MFNP-Tz.

The labeling strategy was further applied to a panel of different bacterial species (Figure 3). Results showed that all Gram-positive species tested showed significantly higher cellular relaxivity values when compared to Gram-negative bacteria. Such magnetic labeling enabled the performance of highly sensitive and rapid detection of Gram-positive bacteria. Titration measurements with serially diluted bacterial samples established that the detection limit with the current experimental setup was approximately 4000 bacteria (Figure S5 in the Supporting Information). This detection method is significantly better than standard UV absorption detection, which has a detection limit of approximately 10^5 bacteria (Figure S6 in the Supporting Information). It is likely that the
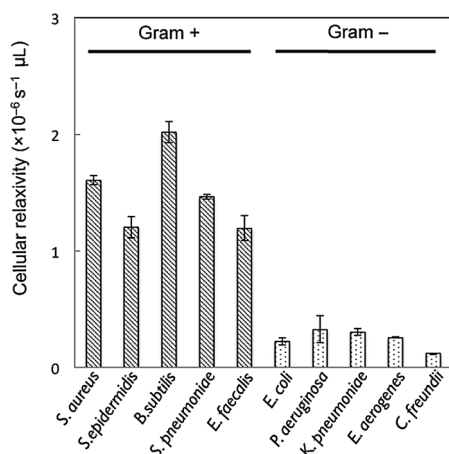

Figure 3. Magnetic detection by μNMR of different species of Gram-positive and Gram-negative bacteria labeled using CV-TCO and MFNP-Tz.

sensitivity of the magnetic detector could be improved to the level of single cells by 1) further miniaturizing the μNMR detection coils, 2) implementing fluidic systems for bacterial enrichment (e.g., membrane filters, magnetic separation steps), and 3) employing different types of magnetic readers (e.g., Hall-effect sensors, giant magnetoresistive sensors).[7–9]

Bioorthogonally labeled bacteria were also analyzed by confocal microscopy using MFNP-Tz (Figure 4A). Bacteria stained with CV-TCO showed uniform and high fluorescence
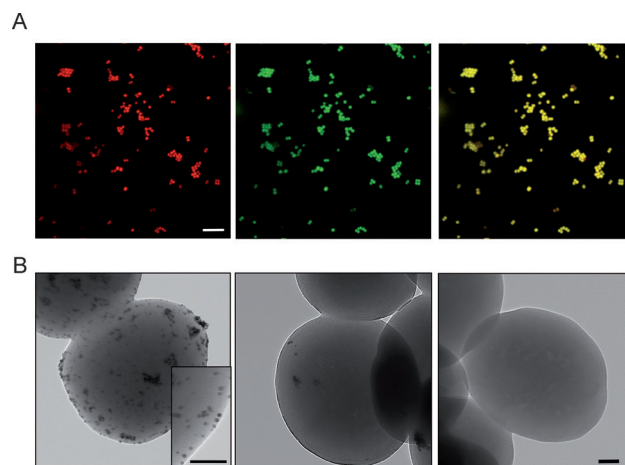

Figure 4. A) Fluorescence confocal microscopy of *S. aureus* stained with CV-TCO and labeled with MFNP-Tz. Left, middle, and right images show images of red channel, green channel, and merged from red and green, respectively (red: propidium iodide for nuclear staining; green: MNFP-Tz staining; scale bar = 10 μm). B) Transmission electron microscopy of *S. aureus* stained with CV-TCO and labeled with AuNP-Tz (left), AuNP-Tz alone (middle), and without any treatment (right; scale bar = 100 nm).

signals in the bacterial cell wall, while the control experiments without CV-TCO showed no signal (Figure S7 in the Supporting Information). Similarly, transmission electron microscopy was performed in bacteria treated with CV-TCO but which were incubated with tetrazine-modified gold nanoparticles (AuNP-Tz). Gold nanoparticles were used instead of magnetic nanoparticles to obtain higher contrast. Gold nanoparticles were found distributed throughout the bacterial surface treated with CV-TCO, while bacteria without CV-TCO labeling showed a smooth surface devoid of nanoparticles (Figure 4B).

By modifying the above procedure, the detection strategy can be applied to detect both Gram-positive and Gram-negative bacteria. Performing the staining without the decolorization process would result in labeling both Gram-positive and negative species, since the Gram-negative species would also retain the CV-TCO (Figure S8A in the Supporting Information). This coloring of both species in the first step is in analogy to the conventional Gram stain where the first staining step "colors" all bacteria and the second decolorization step allows differentiation between the two Gram classes. μNMR measurements showed that before decolorization, both Gram-positive and negative bacteria could be magnetically labeled and detected, while after decolorization, only

Gram-positive species retained their signals (Figure S8B in the Supporting Information). Through these sequential measurements, it is thus possible to obtain total bacterial counts (i.e. detection before decolorization) as well as their Gram-negative and Gram-positive composition (i.e. detection after decolorization).

In summary, we show that an orthogonal CV can be used to detect and broadly classify bacteria in biological samples. Staining bacteria with CV-TCO using the standard Gram stain procedure, followed by labeling with MFNP-Tz allows the detection and characterization of bacteria both by µNMR as well as by optical imaging. The "magnetic Gram stain" could be potentially implemented into automated point-of-care diagnostics, bacterial enrichment for subsequent analysis, as well as into therapeutic applications that utilize the antibacterial, antifungal, and antihelminthic properties of CV. The method could also be used to label bacteria in vivo for various imaging applications.[9] Moreover, the staining strategy presented could be further extended to other small molecule affinity ligands (e.g., bioorthogonal carbol fuchsin or trehalose for mycobacterial species) to enable either universal or specific detection of other bacterial targets. This ability will not only facilitate the clinical diagnosis of a range of bacterial infections but will also promote advances in basic microbiological research.

[1] J. Van Heijenoort, *Glycobiology* **2001**, *11*, 25R–36R.
[2] R. Coico, *Curr. Protocols Immunol.* **2001**, *23*, A.3O.1–A.3O.2.
[3] T. J. Beveridge, *Biotech. Histochem.* **2001**, *76*, 111–118.
[4] J. W. Bartholomew, T. Mittwer, *Bacteriol. Rev.* **1952**, *16*, 1–29.
[5] E. J. Bottone, *Lab. Med.* **1988**, *19*, 288–291.
[6] D. Issadore, H. Shao, J. Chung, A. Newton, M. Pittet, R. Weissleder, H. Lee, *Lab Chip* **2011**, *11*, 147–151.
[7] H. J. Chung, T. Reiner, G. Budin, M. Liong, D. Issadore, H. Lee, R. Weissleder, *ACS Nano* **2011**, *5*, 8834–8841.
[8] M. Liong, M. Fernandez-Suarez, D. Issadore, C. Min, C. Tassa, T. Reiner, S. M. Fortune, M. Toner, H. Lee, R. Weissleder, *Bioconjugate Chem.* **2011**, *22*, 2390–2394.
[9] P. Panizzi, M. Nahrendorf, J-L. Figueiredo, J. Panizzi, B. Marinelli, Y. Iwamoto, E. Keliher, A. A. Maddur, P. Waterman, H. K. Kroh, F. Leuschner, E. Aikawa, F. K. Swirski, M. J. Pittet, T. M. Hackeng, P. Fuentes-Prior, O. Schneewind, P. E. Bock, R. Weissleder, *Nat. Med.* **2011**, *17*, 1142–1146.
[10] Y. Li, M. Castro, H. Im, X. Yao, S.-H. Oh, W.-S. Hu, J.-P. Wang, *J. Med. Devices* **2008**, *2*, 027529.
[11] P. Lönnbro, P. Nordenfelt, H. Tapper, *BMC Cell Biol.* **2008**, *9*, 35.
[12] K. Yang, D. M. Jenkins, W. W. Su, *J. Microbiol. Methods* **2011**, *86*, 69–77.
[13] D. Guillebault, M. Laghdass, P. Catala, I. Obernosterer, P. Lebaron, *Appl. Environ. Microbiol.* **2010**, *76*, 7352.
[14] Y. Zhang, M. Yang, M. Ozkan, C. S. Ozkan, *Biotechnol. Prog.* **2009**, *25*, 923.
[15] R. C. Chaves, D. Bensimon, P. P. Freitas, *J. Appl. Phys.* **2011**, *109*, 064702.
[16] D. Guzmán-Lucero, J. Guzmán, D. Likhatchev, R. Martínez-Palou, *Tetrahedron Lett.* **2005**, *46*, 1119–1122.